

The topological Hubbard model and its high-temperature quantum Hall effect

Titus Neupert,¹ Luiz Santos,² Shinsei Ryu,³ Claudio Chamon,⁴ and Christopher Mudry¹

¹*Condensed Matter Theory Group, Paul Scherrer Institute, CH-5232 Villigen PSI, Switzerland*

²*Department of Physics, Harvard University, 17 Oxford Street, Cambridge, Massachusetts 02138, USA*

³*Department of Physics, University of Illinois at Urbana-Champaign,
1110 W. Green Street, Urbana, Illinois 61801-3080, USA*

⁴*Physics Department, Boston University, Boston, Massachusetts 02215, USA*

(Dated: November 23, 2022)

The quintessential two-dimensional lattice model that describes the competition between the kinetic energy of electrons and their short-range repulsive interactions is the repulsive Hubbard model. We study a time-reversal symmetric variant of the repulsive Hubbard model defined on a planar lattice: Whereas the interaction is unchanged, any fully occupied band supports a quantized spin Hall effect. We show that at 1/2 filling of this band, the ground state develops spontaneously and simultaneously Ising ferromagnetic long-range order *and* a quantized charge Hall effect when the interaction is sufficiently strong. We ponder on the possible practical applications, beyond metrology, that the quantized charge Hall effect might have if it could be realized at high temperatures and without external magnetic fields in strongly correlated materials.

I. INTRODUCTION

High-temperature superconductivity¹ and the quantum Hall effect (QHE)² have been two of the central problems in condensed matter physics of the last three decades. The former is related to electrons hopping on a two-dimensional (2D) lattice close to (but not at) half-filling, while the latter focuses on fermions in doped semiconductor heterostructures or graphene in a high magnetic field. High-temperature superconductors are strongly interacting systems, with the potential energy about an order of magnitude larger than the kinetic energy. In the QHE, the kinetic energy is quenched by the external magnetic field. Moreover, interactions are important only in understanding the fractional QHE but not in understanding the integer QHE (IQHE).

The possibility that the IQHE could arise in a lattice Hamiltonian without the Landau levels induced by a uniform magnetic field was suggested by Haldane in 1988³. The essence is that, despite the absence of a uniform magnetic field, the system still lacks time-reversal symmetry. More recently, it was shown that the fractional QHE could also emerge in flat topological bands when they are partially filled^{4–9}. These recent developments point to a natural marriage between the QHE and strongly correlated lattice systems at high filling fraction.

In this paper we study a quintessential strongly correlated lattice 2D system but with a twist. We consider a time-reversal symmetric fermionic Hubbard model in the limit of large onsite repulsion U compared to the bandwidth W of the hopping dispersion, but with hopping terms yielding topologically non-trivial Bloch bands in that they each support a quantized spin Hall conductivity when fully occupied¹⁰. The time-reversal symmetric Hubbard model with a single half-filled nested Bloch band has a charge insulating ground state that supports anti-ferromagnetic long-range order¹. In contrast, the ground state of our time-reversal symmetric Hubbard model with topologically non-trivial Bloch bands *simul-*

taneously displays Ising ferromagnetic long-range order *and* the IQHE at some commensurate filling fraction. The energy scales that can be attained in lattice models are typically rather high, of the order of atomic magnitudes, i.e., electronvolt. If an interacting system with topological bands can be found so as to display the IQHE at high temperatures, it could be of practical use, as we shall explain after we substantiate our claims.

II. STUDY OF THE HUBBARD MODEL

We consider spinful electrons hopping on a bipartite square lattice $\Lambda = A \cup B$ with sublattices A and B , where each sublattice has $N := L_x \times L_y$ sites. The Hubbard Hamiltonian with repulsive interactions ($U > 0$) can be written

$$H := \sum_{\mathbf{k} \in \text{BZ}} c_{\mathbf{k}}^{\dagger} \mathcal{H}_{\mathbf{k}} c_{\mathbf{k}} + U \sum_{\mathbf{r}} \sum_{\alpha=A,B} n_{\mathbf{r},\uparrow,\alpha} n_{\mathbf{r},\downarrow,\alpha}. \quad (2.1a)$$

The component $c_{\mathbf{k},\sigma,\alpha}^{\dagger}$ of the operator-valued spinor $c_{\mathbf{k}}^{\dagger}$ creates an electron with momentum \mathbf{k} from the Brillouin zone (BZ) of sublattice A and with spin $\sigma = \uparrow, \downarrow$, whose Fourier transform $c_{\mathbf{r},\sigma,\alpha}^{\dagger} = N^{-1/2} \sum_{\mathbf{k} \in \text{BZ}} e^{-i\mathbf{k} \cdot \mathbf{r}} c_{\mathbf{k},\sigma,\alpha}^{\dagger}$ is exclusively supported on sublattice $\alpha = A, B$. The 4×4 Hermitean matrix $\mathcal{H}_{\mathbf{k}}$ obeys time-reversal symmetry

$$\mathcal{H}_{+\mathbf{k}} = \sigma_2 \mathcal{H}_{-\mathbf{k}}^* \sigma_2, \quad (2.1b)$$

and, owing to the strong spin-orbit coupling, the residual spin-1/2 $U(1)$ symmetry

$$\mathcal{H}_{+\mathbf{k}} = \sigma_3 \mathcal{H}_{+\mathbf{k}} \sigma_3 \equiv \begin{pmatrix} h_{\mathbf{k}}^{(\uparrow)} & 0 \\ 0 & h_{\mathbf{k}}^{(\downarrow)} \end{pmatrix}, \quad (2.1c)$$

where the Pauli matrices σ_1 , σ_2 , and σ_3 act on the electronic spin-1/2 degrees of freedom. Hence, the two 2×2

Hermitean matrices $h_{\mathbf{k}}^{(\sigma)}$ with $\sigma = \uparrow, \downarrow$ obey

$$h_{+\mathbf{k},\alpha\beta}^{(\uparrow)} = h_{-\mathbf{k},\beta\alpha}^{(\downarrow)}, \quad \forall \mathbf{k} \in \text{BZ}, \quad \alpha, \beta = A, B, \quad (2.1d)$$

because of the condition of time-reversal symmetry (2.1b). Finally, the operator $n_{\mathbf{r},\sigma,\alpha} = c_{\mathbf{r},\sigma,\alpha}^\dagger c_{\mathbf{r},\sigma,\alpha}$ measures the electron density on site \mathbf{r} in sublattice α and with spin σ .

It is the choice for the matrix elements $h_{\mathbf{k},\alpha\beta}^{(\sigma)}$ entering the kinetic energy (2.1c) that endows the Hubbard Hamiltonian (2.1) with topological attributes. We choose

$$\begin{aligned} h_{\mathbf{k},AB}^{(\uparrow)} &= h_{\mathbf{k},BA}^{(\uparrow)*} := w_{\mathbf{k}} \left[e^{-i\pi/4} \left(1 + e^{+i(k_y - k_x)} \right) \right. \\ &\quad \left. + e^{+i\pi/4} \left(e^{-ik_x} + e^{+ik_y} \right) \right], \\ h_{\mathbf{k},AA}^{(\uparrow)} &= -h_{\mathbf{k},BB}^{(\uparrow)} := w_{\mathbf{k}} \left[2t_2(\cos k_x - \cos k_y) + 4\mu_s \right], \end{aligned} \quad (2.2a)$$

where

$$w_{\mathbf{k}}^{-1} := \kappa \varepsilon_{\mathbf{k}} + (1 - \kappa), \quad \kappa \in [0, 1], \quad (2.2b)$$

and

$$\varepsilon_{\mathbf{k}} := \sqrt{1 + \cos k_x \cos k_y + [2t_2(\cos k_x - \cos k_y) + 4\mu_s]^2}. \quad (2.2c)$$

In the non-interacting limit ($U = 0$), this model features four bands with two distinct two-fold degenerate dispersions $\pm w_{\mathbf{k}} \varepsilon_{\mathbf{k}}$, i.e., the eigenvalues of $h_{\mathbf{k}}^{(\sigma)} \equiv \left(h_{\mathbf{k},\alpha\beta}^{(\sigma)} \right)^4$. The two-fold degeneracy arises due to the residual $U(1)$ spin-rotation symmetry (2.1c). If we denote the corresponding eigenspinors $\chi_{\mathbf{k},\sigma,\lambda} = (\chi_{\mathbf{k},\sigma,\lambda,\alpha})$ where $\lambda = \pm$ and choose the normalization $\chi_{\mathbf{k},\sigma,\lambda}^\dagger \chi_{\mathbf{k},\sigma,\lambda'} = \delta_{\lambda,\lambda'}$, $\forall \mathbf{k}$, then the kinetic energy is diagonalized using the fermionic creation operators

$$d_{\mathbf{k},\sigma,\lambda}^\dagger := \sum_{\alpha=A,B} \chi_{\mathbf{k},\sigma,\lambda,\alpha}^* c_{\mathbf{k},\sigma,\alpha}^\dagger, \quad (2.2d)$$

as

$$H_0 := \sum_{\mathbf{k} \in \text{BZ}} \sum_{\sigma=\uparrow,\downarrow} \sum_{\lambda=\pm} \lambda d_{\mathbf{k},\sigma,\lambda}^\dagger w_{\mathbf{k}} \varepsilon_{\mathbf{k}} d_{\mathbf{k},\sigma,\lambda}. \quad (2.2e)$$

Hence, the Bloch states created by $d_{\mathbf{k},\sigma,\lambda}^\dagger$ are generically spread on both sublattices A and B . We shall only consider the case in which these bands are separated by an energy gap, i.e., $|t_2| \neq |\mu_s|$. The parameter κ controls the bandwidth of these bands. For $\kappa = 1$, the bands are exactly flat with eigenvalues ± 1 . The case $\kappa = 0$ corresponds to a tight-binding model on the square lattice that involves only nearest-neighbor ($|t_1| = 1$) and next-nearest-neighbor hopping (t_2) together with a staggered chemical potential μ_s that breaks the symmetry between sublattices A and B ⁴. For $\kappa \in (0, 1]$ longer range hopping is introduced. However, we stress that the Hamiltonian

remains local for all $\kappa \in [0, 1]$ since all correlation functions decay exponentially due to the presence of the band gap⁴.

The topological properties of the lower pair of bands are characterized by their spin Chern number

$$C_s := (C_\uparrow - C_\downarrow) / 2, \quad (2.3a)$$

where C_σ is to be computed from the orbitals of spin- σ electrons according to

$$C_\sigma := \int_{\mathbf{k} \in \text{BZ}} \frac{d^2 \mathbf{k}}{2\pi i} \nabla_{\mathbf{k}} \wedge \left(\chi_{\mathbf{k},\sigma,-}^\dagger \nabla_{\mathbf{k}} \chi_{\mathbf{k},\sigma,-} \right). \quad (2.3b)$$

Time reversal symmetry implies $C_\uparrow = -C_\downarrow$ and therefore entails a vanishing of the total (charge) Chern number $C_c := (C_\uparrow + C_\downarrow) / 2$ of the lower bands. The spin Chern number of the lower pair of bands is given by

$$C_s = \frac{1}{2} \left(\text{sgn} h_{(0,\pi),AA}^{(\uparrow)} - \text{sgn} h_{(\pi,0),AA}^{(\uparrow)} \right). \quad (2.3c)$$

Hence, the Bloch bands are topologically trivial whenever $|t_2/\mu_s| < 1$, while the model at half filling exhibits the physics of a quantum spin Hall insulator whenever $|t_2/\mu_s| > 1$. In an open geometry, the spin Hall conductivity is quantized to the value $\sigma_{xy}^{\text{SH}} = eC_s/(2\pi)$ where e denotes the electric charge of the electron.

We now consider the system with a repulsive Hubbard interaction $U > 0$ at $1/2$ filling of the lower band ($1/4$ filling of the lower and upper bands), i.e., with

$$N_e = L_x \times L_y = N \quad (2.4)$$

electrons. In all what follows, we assume that U is much smaller than the gap Δ_0 between the two pairs of bands. If so, we can restrict the N_e -body Hilbert space to the Fock space arising from the single-particle Hilbert spaces of the lower pair of bands.

In the limit of flat bands $\kappa = 1$ and at the commensurate filling fraction (2.4), the kinetic energy (2.2e) at fixed spin polarization $S := |\langle \sigma_3 \rangle| = 0, 2, \dots, N$ in units of $\hbar/2$ has a ground state degeneracy

$$\mathcal{N}_{\text{gs}} = \binom{N}{\frac{N-|S|}{2}}. \quad (2.5)$$

The repulsive Hubbard interaction lifts this degeneracy whenever any one of these states allows a site of Λ to be doubly occupied with a finite probability. The only two states with full spin-polarization $S = N$

$$|\Psi_\sigma\rangle = \prod_{\mathbf{k} \in \text{BZ}} d_{\mathbf{k},\sigma,-}^\dagger |0\rangle, \quad \sigma = \uparrow, \downarrow, \quad (2.6a)$$

are immune to the presence of the Hubbard repulsion. More formally, observe that Hamiltonian $H - \mu N_e$ is a positive semidefinite operator for $\kappa = 1$, $U > 0$, and the chemical potential $\mu = -1$. Since

$$\langle \Psi_\sigma | (H + N_e) | \Psi_\sigma \rangle = 0, \quad \sigma = \uparrow, \downarrow, \quad (2.6b)$$

the two states (2.6a) belong to the ground state manifold of $H + N_e$ for any $U > 0$, t_2 , and μ_s .

We are going to argue that this pair of degenerate Ising ferromagnets spans the ground state manifold for any $U > 0$ and $|t_2/\mu_s| \neq 1$. This is achieved by arguing that they are separated from excited states by a many-body gap, a departure from the usual ferromagnetism in flat bands when full spin-1/2 $SU(2)$ symmetry is not explicitly broken¹¹. First, particle-hole excitations of $|\Psi_\sigma\rangle$ that keep $S = N$ fixed, cost an energy $\Delta_0 > 0$ and are thus gaped. Second, we ask whether excitations of $|\Psi_\sigma\rangle$ that flip one spin ($S = N - 2$) are gaped as well. Any such state can be written as

$$|\Phi_{\sigma,\mathbf{Q}}\rangle = \sum_{\mathbf{k} \in \text{BZ}} A_{\mathbf{k}}^{(\mathbf{Q})} d_{\mathbf{k}+\mathbf{Q},\bar{\sigma},-}^\dagger d_{\mathbf{k},\sigma,-} |\Psi_\sigma\rangle, \quad \sigma = \uparrow, \downarrow, \quad (2.7a)$$

where the center of mass momentum \mathbf{Q} is a good quantum number and thus $\langle \Phi_{\sigma,\mathbf{Q}} | \Phi_{\sigma,\mathbf{Q}'} \rangle = \delta_{\mathbf{Q},\mathbf{Q}'}$ if the normalization $\sum_{\mathbf{k} \in \text{BZ}} A_{\mathbf{k}}^{(\mathbf{Q})*} A_{\mathbf{k}}^{(\mathbf{Q})} = 1$ is imposed. One verifies that (see Appendix)

$$\begin{aligned} & \langle \Phi_{\sigma,\mathbf{Q}} | (H + N_e) | \Phi_{\sigma,\mathbf{Q}} \rangle \\ &= U - \frac{U}{N} \sum_{\alpha} \left| \sum_{\mathbf{k} \in \text{BZ}} A_{\mathbf{k}}^{(\mathbf{Q})} \chi_{-\mathbf{k}-\mathbf{Q},\sigma,-,\alpha} \chi_{\mathbf{k},\sigma,-,\alpha} \right|^2, \end{aligned} \quad (2.7b)$$

where the lowest energy state with one spin flipped is characterized by the $A_{\mathbf{k}}^{(\mathbf{Q})}$ that minimizes Eq. (2.7b) while satisfying the normalization condition. For example, if the single-particle orbitals are fully sublattice polarized, e.g., $\chi_{\mathbf{k},\sigma,-} \propto (1, 0)$ (topologically trivial), the choice $A_{\mathbf{k}}^{(\mathbf{Q})} = N^{-1/2}$ minimizes Eq. (2.7b) with the right-hand side equal to zero. Hence, the fully spin-polarized state $|\Psi_\sigma\rangle$ is a *gapless* ground state in this case. On the other hand, let us assume that

$$\chi_{\mathbf{k},\sigma,-}^\dagger \not\propto (1, 0) \quad \text{and} \quad \chi_{\mathbf{k},\sigma,-}^\dagger \not\propto (0, 1) \quad (2.8)$$

holds almost everywhere in the BZ, i.e., up to a set of measure zero. In the thermodynamic limit, where the sum over \mathbf{k} becomes an integral, this delivers from Eq. (2.7b) the *strict* inequality (see Appendix)

$$\langle \Phi_{\sigma,\mathbf{Q}} | (H + N_e) | \Phi_{\sigma,\mathbf{Q}} \rangle > 0. \quad (2.9)$$

Hence, assumption (2.8) is sufficient to show that the spin-polarized state $|\Psi_\sigma\rangle$ is a *gaped* ground state of the Hamiltonian with flat bands in the thermodynamic limit, provided that one assumes that the lowest energy states with more than one spin flipped are higher in energy than those with one spin flipped. Equation (2.8) is a reasonable assumption when the Bloch states stem from a band with non-zero (spin) Chern number, since the spinor $\chi_{\mathbf{k},\sigma}$ maps out the entire surface of the unit sphere as \mathbf{k} takes values in the BZ.

The assumption underlying Eq. (2.8) can also be understood by constructing the Wannier wavefunctions,

centered at the lattice point \mathbf{z} , of the lowest energy band with spin σ and Chern number C_σ

$$\psi_{\mathbf{z},\mathbf{r},\sigma,-,\alpha} := \frac{1}{N} \sum_{\mathbf{k} \in \text{BZ}} e^{i\mathbf{k} \cdot (\mathbf{r}-\mathbf{z})} \chi_{\mathbf{k},\sigma,-,\alpha}. \quad (2.10a)$$

The gauge invariant part of their spread functional¹² satisfies

$$\begin{aligned} & \langle \psi_{0,\sigma,-} | \mathbf{r}^2 | \psi_{0,\sigma,-} \rangle - \sum_{\mathbf{z}} |\langle \psi_{0,\sigma,-} | \mathbf{r} | \psi_{\mathbf{z},\sigma,-} \rangle|^2 \\ & \geq |C_\sigma| \mathcal{A}_c / (2\pi), \end{aligned} \quad (2.10b)$$

where \mathcal{A}_c denotes the area of the unit cell. This inequality relates the Chern number of the band and the ‘‘minimum width’’ of the Wannier states (see Appendix). In particular, in the non-topological phase, one can imagine a limit in which the wavefunction is entirely localized on a given sublattice, while the non-zero Chern number in the topological phase implies that the Wannier wavefunction has amplitudes on both sublattices.

While Eq. (2.9) is strongly suggestive of the existence of a many-body gap Δ , it does not provide information about its size. To quantify Δ , we diagonalized the model (2.1) exactly numerically in the limit of flat bands $\kappa = 1$ at the commensurate filling fraction (2.4). We varied the ratio $|t_2/\mu_s|$, keeping $t_2^2 + \mu_s^2 = 1/2$ constant to drive the system from the topological to the trivial phase. The results are shown in Fig. 1. First, they support the assumption that all states with more than one spin flipped are higher in energy than the many-body one-spin-flipped gap provided $|t_2/\mu_s| > 1$. Second, we find $\Delta \approx 0.3U$ as an extrapolation to the thermodynamic limit for $\mu_s = 0$ deep in the topological phase, while Δ monotonously decreases toward a much smaller non-vanishing value for $t_2 = 0$ in the topologically trivial phase set by the unit of energy $|t_1| = 1$. Finally, it should be noted that neglecting the states from the upper band of the non-interacting Hamiltonian delivers the correct excitation many-body gap Δ not only in the aforementioned limit $U \ll \Delta_0$, but also under the weaker condition $\Delta < \Delta_0$, if the limit of flat bands is taken.

Deep in the topologically non-trivial regime $|t_2/\mu_s| \gg 1$, the states $|\Psi_\sigma\rangle$ and $|\Psi_{\bar{\sigma}}\rangle$ are degenerate ground states related by time-reversal symmetry for any finite N . They are separated from their excitations by a gap that survives the thermodynamic limit $N \rightarrow \infty$. Spontaneous breaking of time-reversal symmetry takes place in the thermodynamic limit $N \rightarrow \infty$ by selecting the ground state to be $|\Psi_\uparrow\rangle$, say. It is then meaningful to discuss the quantized electromagnetic response of $|\Psi_\uparrow\rangle$ since time-reversal symmetry is spontaneously broken. The transverse charge response σ_{xy}^H of $|\Psi_\uparrow\rangle$ is proportional to the many-body Chern number $C_{|\Psi_\uparrow\rangle}$. The latter takes into account the occupation of the Bloch states⁴. Since all Bloch states of the lower band with spin σ are occupied in $|\Psi_\uparrow\rangle$, while all Bloch states with spin \downarrow are empty,

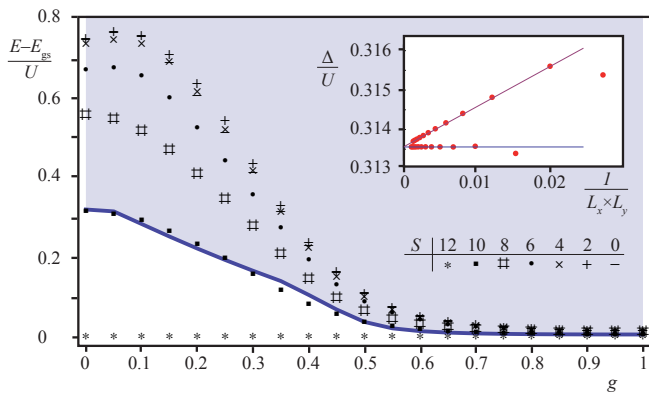


FIG. 1. Numerical exact diagonalization results for flat bands $\kappa = 1$ at the commensurate filling fraction (2.4). Markers show the energy of the lowest state in different sectors of total spin S (in units of $\hbar/2$) measured with respect to the ground state energy for $L_x = 3$, $L_y = 4$. Here, $g := (2/\pi)\arctan|\mu_s/t_2|$ so that $g > 0.5$ and $g < 0.5$ correspond to the trivial and topological single-particle bands, respectively. Since there is only one state in the fully polarized sector $|S| = 12$, the difference between the asterisks and the squares is the many-body excitation gap $\Delta(g)$. The thick blue line shows the extrapolation of $\Delta(g)$ to the thermodynamic limit. In the inset, exact diagonalization in the sector with one spin flipped away from the fully polarized sector is presented for $\mu_s = 0$, $t_2 = 1/\sqrt{2}$ and $L_x = L_y$ ranging from 6 to 30. The straight lines are guide to the eye and make evident an even-odd effect in $L_x = L_y$. Deep in the topologically non-trivial regime $g \ll 0.5$, we observe a sizable $\Delta(g \ll 0.5)$. The topologically trivial regime $g > 0.5$ is also characterized by a gap $\Delta(g > 0.5)$ in the sector with one spin flipped away from the fully polarized sector, however this gap is much smaller than $\Delta(g \ll 0.5)$. We refer the reader to the Appendix for a discussion of the regime $\Delta(g > 0.5)$.

$C_{|\Psi_\uparrow\rangle} \equiv C_\uparrow$. Hence, the ground state has the quantized Hall response

$$|\sigma_{xy}^H| = |C_\uparrow| \times e^2/h = e^2/h. \quad (2.11)$$

Remarkably, the selection by the repulsive Hubbard interaction of a ground state supporting *simultaneously* Ising ferromagnetism *and* the IQHE is robust to a sizable bandwidth as is suggested by numerical exact diagonalization. As shown in Fig. (2), the fully spin-polarized state $|\Psi_\sigma\rangle$ remains the gaped ground state of the system up to a bandwidth $W/U \approx 0.7$.

III. PRACTICAL APPLICATIONS

So what is it good for, a material with a QHE at high temperature without applied external magnetic fields? The IQHE has already a very practical application in metrology, defining the standard for resistance $R_K = h/e^2 = 25813.807\dots\Omega$ using the quantized transverse Hall resistance^{13,14}. However, one may ponder if one could explore the fact that the longitudinal resistance

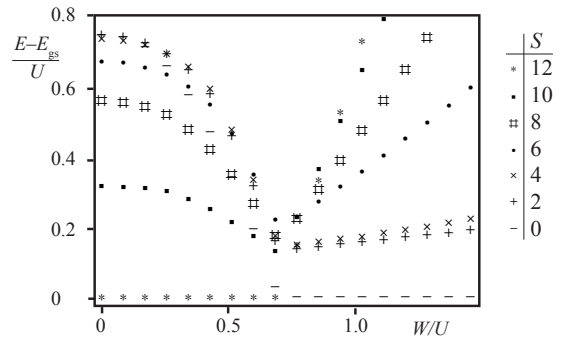


FIG. 2. (Color online) Numerical exact diagonalization results at the commensurate filling fraction (2.4) as a function of the bandwidth W for $L_x = 3$, $L_y = 4$. Plotted is the energy of the lowest state in different sectors of total spin S (in units of $\hbar/2$) measured with respect to the ground state energy in the topological phase with $\mu_s = 0$, $t_2 = 1/\sqrt{2}$. The ground state is gaped and fully spin-polarized for $W/U < 0.7$, while it is unpolarized for $W/U > 0.7$.

vanishes while the transverse conductance becomes quantized, and make use of this form of dissipationless transport in practical applications. In the absence of a room temperature superconductor, could a low longitudinal resistivity system play runner-up?

To address these questions, first one has to be clear that in a superconductor the resistance is *equal* to zero below the superconducting transition temperature T_c , while the longitudinal resistance in the QHE is exponentially suppressed with temperature, and vanishes in principle only at absolute zero temperature¹⁴. But if a QHE with gaps of the order of hundreds of meV even eV scales could arise in a strongly correlated lattice material, exceptionally low resistivities could be attained. The resistance of a Hall bar depends on its aspect ratio and the Hall angle $\delta = \arctan(\rho_{xy}/\rho_{xx})$ ¹⁵, but for long systems (“wires”) near the quantized regime, the longitudinal resistance scales as $R_{xx} = L/W \rho_{xx}$, and the two-dimensional resistivity $\rho_{xx} \sim R_K e^{-\Delta/T}$, where Δ is the excitation gap. For gaps of the order of 100 meV to 1 eV, one would obtain room temperature 2D resistivities from $\rho_{xx} \sim 10^3 \Omega$ to $\rho_{xx} \sim 10^{-13} \Omega$, respectively. Obviously the exponential behavior is responsible for this gigantic range. Small as they are, these are not perfect conductors.

For a benchmark, we consider the conductivity of copper at room temperature. More precisely, we consider the conductivity of copper per atomic layer, for the right comparison with a layered lattice material displaying the QHE should be per layer. Using the value for the 3D resistivity of copper at 20°C of $\rho_{Cu}^{3D} = 1.68 \times 10^{-8} \Omega \text{ m}$ ¹⁶ and that the lattice parameter for FCC lattice is 3.61Å, we obtain $\rho_{Cu}^{2D} = 93.3 \Omega$. Therefore, for gaps above $\Delta \approx .2 \text{ eV}$, the Hall system starts to be better conducting than copper at room temperature, and for $\Delta \approx .3 \text{ eV}$ it is already almost three orders of magnitude better conducting than copper.

We would like to close by mentioning that examples

such as the topological Hubbard model discussed in this Letter, as well as lattice models displaying the FQHE studied in Refs. 4–7, could serve as benchmarks for numerical methods of fermionic models in two-dimensions such as Dynamical Mean-Field Theory (DMFT) and methods based on Tensor Product States (TPS)¹⁷. In contrast to the single-band repulsive Hubbard model, for which little is known exactly at fractional filling, the topological Hubbard model (2.1), because of the non-vanishing Chern numbers of its bands, leads to much better understood (topological) ground states. It can thus serve as a yardstick for the performance of these methods.

Appendix A: Intermediary steps

1. Derivation of Eq. (2.7b)

For the limit of flat bands $\kappa = 1$, we are going to compute the expectation value

$$\langle \Phi_{\sigma, \mathbf{Q}} | (H + N_e) | \Phi_{\sigma, \mathbf{Q}} \rangle \quad (\text{A1a})$$

in the N_e -many-body state

$$|\Phi_{\sigma, \mathbf{Q}}\rangle = \sum_{\mathbf{k} \in \text{BZ}} A_{\mathbf{k}}^{(\mathbf{Q})} d_{\mathbf{k}+\mathbf{Q}, \bar{\sigma}, -}^\dagger d_{\mathbf{k}, \sigma, -} |\Psi_\sigma\rangle, \quad \sigma = \uparrow, \downarrow, \quad (\text{A1b})$$

which has one spin flipped as compared to the – up to time-reversal symmetry and the global gauge phase factor – unique normalized N_e -many-body state with full spin polarization

$$|\Psi_\sigma\rangle = \prod_{\mathbf{k} \in \text{BZ}} d_{\mathbf{k}, \sigma, -}^\dagger |0\rangle, \quad \sigma = \uparrow, \downarrow. \quad (\text{A1c})$$

Here, \mathbf{Q} denotes the center of mass momentum and the orthonormalization condition

$$\langle \Phi_{\sigma, \mathbf{Q}} | \Phi_{\sigma, \mathbf{Q}'} \rangle = \delta_{\mathbf{Q}, \mathbf{Q}'} \quad (\text{A1d})$$

enforces the normalization

$$\sum_{\mathbf{k} \in \text{BZ}} A_{\mathbf{k}}^{(\mathbf{Q})*} A_{\mathbf{k}}^{(\mathbf{Q})} = 1. \quad (\text{A1e})$$

This work was supported in part by DOE Grant DEFG02-06ER46316 and by the Swiss National Science Foundation.

We rewrite $|\Phi_{\sigma, \mathbf{Q}}\rangle$ as

$$\begin{aligned} |\Phi_{\sigma, \mathbf{Q}}\rangle &= \sum_{\mathbf{k} \in \text{BZ}} A_{\mathbf{k}}^{(\mathbf{Q})} \left(\sum_{\alpha=A, B} \chi_{\mathbf{k}+\mathbf{Q}, \bar{\sigma}, -}^* c_{\mathbf{k}+\mathbf{Q}, \bar{\sigma}, \alpha}^\dagger \right) \left(\sum_{\beta=A, B} \chi_{\mathbf{k}, \sigma, -} c_{\mathbf{k}, \sigma, \beta} \right) |\Psi_\sigma\rangle \\ &= \sum_{\alpha, \beta=A, B} \sum_{\mathbf{r}, \mathbf{r}' \in A} \left[\sum_{\mathbf{k} \in \text{BZ}} \frac{A_{\mathbf{k}}^{(\mathbf{Q})}}{N} \chi_{\mathbf{k}+\mathbf{Q}, \bar{\sigma}, -}^* \chi_{\mathbf{k}, \sigma, -} e^{-i(\mathbf{k}+\mathbf{Q}) \cdot \mathbf{r}} e^{i\mathbf{k} \cdot \mathbf{r}'} \right] c_{\mathbf{r}, \bar{\sigma}, \alpha}^\dagger c_{\mathbf{r}', \sigma, \beta} |\Psi_\sigma\rangle \\ &\equiv \sum_{\alpha, \beta=A, B} \sum_{\mathbf{r}, \mathbf{r}' \in A} M_{\mathbf{r}, \alpha, \mathbf{r}', \beta}^{(\sigma)} c_{\mathbf{r}, \bar{\sigma}, \alpha}^\dagger c_{\mathbf{r}', \sigma, \beta} |\Psi_\sigma\rangle, \end{aligned} \quad (\text{A2a})$$

where we have introduced the short-hand notation

$$M_{\mathbf{r}, \alpha, \mathbf{r}', \beta}^{(\sigma)} := \sum_{\mathbf{k} \in \text{BZ}} \frac{A_{\mathbf{k}}^{(\mathbf{Q})}}{N} \chi_{\mathbf{k}+\mathbf{Q}, \bar{\sigma}, -}^* \chi_{\mathbf{k}, \sigma, -} e^{-i(\mathbf{k}+\mathbf{Q}) \cdot \mathbf{r}} e^{i\mathbf{k} \cdot \mathbf{r}'}. \quad (\text{A2b})$$

in terms of which

$$\begin{aligned}
\langle \Phi_{\uparrow, \mathbf{Q}} | (H + N_e) | \Phi_{\uparrow, \mathbf{Q}} \rangle &= U \sum_{\tilde{\mathbf{r}} \in A} \sum_{\delta=A, B} \langle \Phi_{\uparrow, \mathbf{Q}} | n_{\tilde{\mathbf{r}}, \uparrow, \delta} n_{\tilde{\mathbf{r}}, \downarrow, \delta} | \Phi_{\uparrow, \mathbf{Q}} \rangle \\
&= U \sum_{\tilde{\mathbf{r}}, \mathbf{r}, \mathbf{r}' \in A} \sum_{\alpha, \beta, \delta=A, B} \left| M_{\mathbf{r}, \alpha, \mathbf{r}', \beta}^{(\uparrow)} \right|^2 \langle \Psi_{\uparrow} | c_{\mathbf{r}', \uparrow, \beta}^{\dagger} c_{\mathbf{r}, \downarrow, \alpha} n_{\tilde{\mathbf{r}}, \uparrow, \delta} n_{\tilde{\mathbf{r}}, \downarrow, \delta} c_{\mathbf{r}, \downarrow, \alpha}^{\dagger} c_{\mathbf{r}', \uparrow, \beta} | \Psi_{\uparrow} \rangle \\
&= U \sum_{\tilde{\mathbf{r}}, \mathbf{r}, \mathbf{r}' \in A} \sum_{\alpha, \beta, \delta=A, B} \left| M_{\mathbf{r}, \alpha, \mathbf{r}', \beta}^{(\uparrow)} \right|^2 (1 - \delta_{\mathbf{r}, \mathbf{r}'} \delta_{\alpha, \beta}) \delta_{\tilde{\mathbf{r}}, \mathbf{r}} \delta_{\delta, \alpha} \\
&= U \sum_{\mathbf{r}, \mathbf{r}' \in A} \sum_{\alpha, \beta=A, B} \left| M_{\mathbf{r}, \alpha, \mathbf{r}', \beta}^{(\uparrow)} \right|^2 - U \sum_{\mathbf{r} \in A} \sum_{\alpha=A, B} \left| M_{\mathbf{r}, \alpha, \mathbf{r}, \alpha}^{(\uparrow)} \right|^2.
\end{aligned} \tag{A3}$$

Using the definition (A2b), the first term becomes

$$\begin{aligned}
\sum_{\mathbf{r}, \mathbf{r}' \in A} \sum_{\alpha, \beta=A, B} \left| M_{\mathbf{r}, \alpha, \mathbf{r}', \beta}^{(\uparrow)} \right|^2 &= \sum_{\mathbf{r}, \mathbf{r}' \in A} \sum_{\alpha, \beta=A, B} \sum_{\mathbf{k}, \mathbf{k}' \in \text{BZ}} \frac{A_{\mathbf{k}}^{(\mathbf{Q})} A_{\mathbf{k}'}^{(\mathbf{Q})*}}{N^2} \chi_{\mathbf{k}+\mathbf{Q}, \downarrow, -\beta}^* \chi_{\mathbf{k}, \uparrow, -\alpha} \chi_{\mathbf{k}'+\mathbf{Q}, \downarrow, -\beta} \chi_{\mathbf{k}', \uparrow, -\alpha} e^{-i(\mathbf{k}-\mathbf{k}') \cdot (\mathbf{r}-\mathbf{r}')} \\
&= \sum_{\alpha, \beta=A, B} \sum_{\mathbf{k}, \mathbf{k}' \in \text{BZ}} \frac{A_{\mathbf{k}}^{(\mathbf{Q})} A_{\mathbf{k}'}^{(\mathbf{Q})*}}{N^2} \chi_{\mathbf{k}+\mathbf{Q}, \downarrow, -\beta}^* \chi_{\mathbf{k}, \uparrow, -\alpha} \chi_{\mathbf{k}'+\mathbf{Q}, \downarrow, -\beta} \chi_{\mathbf{k}', \uparrow, -\alpha} N^2 \delta_{\mathbf{k}, \mathbf{k}'} \\
&= \sum_{\mathbf{k}, \mathbf{k}' \in \text{BZ}} A_{\mathbf{k}}^{(\mathbf{Q})} A_{\mathbf{k}'}^{(\mathbf{Q})*} \left(\sum_{\beta=A, B} \chi_{\mathbf{k}+\mathbf{Q}, \downarrow, -\beta}^* \chi_{\mathbf{k}, \uparrow, -\alpha} \right) \left(\sum_{\alpha=A, B} \chi_{\mathbf{k}, \uparrow, -\alpha} \chi_{\mathbf{k}+\mathbf{Q}, \downarrow, -\beta} \right) \\
&= \sum_{\mathbf{k}, \mathbf{k}' \in \text{BZ}} A_{\mathbf{k}}^{(\mathbf{Q})} A_{\mathbf{k}'}^{(\mathbf{Q})*} \\
&= 1,
\end{aligned} \tag{A4}$$

where both the normalization conditions on $A_{\mathbf{k}}^{(\mathbf{Q})}$ in Eq. (A1e) and on $\chi_{\mathbf{k}, \sigma, -\alpha}$ have been used in the last two lines. The second term in Eq. (A3) becomes

$$\begin{aligned}
\sum_{\mathbf{r} \in A} \sum_{\alpha=A, B} \left| M_{\mathbf{r}, \alpha, \mathbf{r}, \alpha}^{(\uparrow)} \right|^2 &= \sum_{\mathbf{r} \in A} \sum_{\alpha=A, B} \sum_{\mathbf{k}, \mathbf{k}' \in \text{BZ}} \frac{A_{\mathbf{k}}^{(\mathbf{Q})} A_{\mathbf{k}'}^{(\mathbf{Q})*}}{N^2} \chi_{\mathbf{k}+\mathbf{Q}, \downarrow, -\alpha}^* \chi_{\mathbf{k}, \uparrow, -\alpha} \chi_{\mathbf{k}'+\mathbf{Q}, \downarrow, -\alpha} \chi_{\mathbf{k}', \uparrow, -\alpha} \\
&= \sum_{\alpha=A, B} \sum_{\mathbf{k}, \mathbf{k}' \in \text{BZ}} \frac{A_{\mathbf{k}}^{(\mathbf{Q})} A_{\mathbf{k}'}^{(\mathbf{Q})*}}{N} \chi_{\mathbf{k}+\mathbf{Q}, \downarrow, -\alpha}^* \chi_{\mathbf{k}, \uparrow, -\alpha} \chi_{\mathbf{k}'+\mathbf{Q}, \downarrow, -\alpha} \chi_{\mathbf{k}', \uparrow, -\alpha} \\
&= \frac{1}{N} \sum_{\alpha=A, B} \left| \sum_{\mathbf{k} \in \text{BZ}} A_{\mathbf{k}}^{(\mathbf{Q})} \chi_{\mathbf{k}+\mathbf{Q}, \downarrow, -\alpha}^* \chi_{\mathbf{k}, \uparrow, -\alpha} \right|^2 \\
&= \frac{1}{N} \sum_{\alpha=A, B} \left| \sum_{\mathbf{k} \in \text{BZ}} A_{\mathbf{k}}^{(\mathbf{Q})} \chi_{-\mathbf{k}-\mathbf{Q}, \uparrow, -\alpha} \chi_{\mathbf{k}, \uparrow, -\alpha} \right|^2,
\end{aligned} \tag{A5}$$

where we used the identity $\chi_{\mathbf{k}, \sigma, \lambda, \alpha} = \chi_{-\mathbf{k}, \bar{\sigma}, \lambda, \alpha}^*$ which follows from the time-reversal symmetry of the Hamiltonian. Putting everything together, we obtain Eq. (2.7b) of the Letter,

$$\langle \Phi_{\sigma, \mathbf{Q}} | (H + N_e) | \Phi_{\sigma, \mathbf{Q}} \rangle = U - \frac{U}{N} \sum_{\alpha=A, B} \left| \sum_{\mathbf{k} \in \text{BZ}} A_{\mathbf{k}}^{(\mathbf{Q})} \chi_{-\mathbf{k}-\mathbf{Q}, \sigma, -\alpha} \chi_{\mathbf{k}, \sigma, -\alpha} \right|^2. \tag{A6}$$

2. Derivation of Eq. (2.9)

Before starting with the derivation of the inequality Eq. (2.9), let us establish the following inequality

$$1 \geq abcd + \sqrt{1-a^2} \sqrt{1-b^2} \sqrt{1-c^2} \sqrt{1-d^2} \tag{A7}$$

for $a, b, c, d \in [0, 1]$. In particular, the equality only holds when either $a = b = c = d = 0$ or $a = b = c = d = 1$. To show this, one can rewrite the inequality in terms of

trigonometric functions with angles $\alpha, \beta, \gamma, \delta \in [0, \pi/2]$

$$\begin{aligned} 1 &\geq \sin \alpha \sin \beta \sin \gamma \sin \delta + \cos \alpha \cos \beta \cos \gamma \cos \delta \\ &= \frac{1}{2} [\cos(\alpha + \beta) \cos(\gamma + \delta) + \cos(\alpha - \beta) \cos(\gamma - \delta)]. \end{aligned} \quad (\text{A8})$$

Hence the inequality holds and the equality is true only if either $\alpha = \beta = \gamma = \delta = 0$ or $\alpha = \beta = \gamma = \delta = \pi/2$ as announced.

We will now show that in the thermodynamic limit the

strict inequality

$$U - \frac{U}{N} \sum_{\alpha=A,B} \left| \sum_{\mathbf{k} \in \text{BZ}} A_{\mathbf{k}}^{(\mathcal{Q})} \chi_{-\mathbf{k}-\mathcal{Q},\sigma,-,\alpha} \chi_{\mathbf{k},\sigma,-,\alpha} \right|^2 > 0 \quad (\text{A9})$$

holds under the assumption that Eq. (2.8) is satisfied almost everywhere in the BZ, i.e., up to a set of measure zero.

We rewrite, for very large N ,

$$\begin{aligned} &\frac{U}{N} \sum_{\alpha=A,B} \left| \sum_{\mathbf{k} \in \text{BZ}} A_{\mathbf{k}}^{(\mathcal{Q})} \chi_{-\mathbf{k}-\mathcal{Q},\sigma,-,\alpha} \chi_{\mathbf{k},\sigma,-,\alpha} \right|^2 \\ &\rightarrow NU \int \frac{d^2 \mathbf{k}}{(2\pi)^2} \int \frac{d^2 \mathbf{k}'}{(2\pi)^2} A_{\mathbf{k}}^{(\mathcal{Q})} A_{\mathbf{k}'}^{(\mathcal{Q})*} \sum_{\alpha=A,B} \chi_{-\mathbf{k}-\mathcal{Q},\sigma,-,\alpha} \chi_{\mathbf{k},\sigma,-,\alpha} \chi_{-\mathbf{k}'-\mathcal{Q},\sigma,-,\alpha}^* \chi_{\mathbf{k}',\sigma,-,\alpha}^* \\ &\leq NU \int \frac{d^2 \mathbf{k}}{(2\pi)^2} \int \frac{d^2 \mathbf{k}'}{(2\pi)^2} |A_{\mathbf{k}}^{(\mathcal{Q})}| |A_{\mathbf{k}'}^{(\mathcal{Q})*}| \sum_{\alpha=A,B} |\chi_{-\mathbf{k}-\mathcal{Q},\sigma,-,\alpha}| |\chi_{\mathbf{k},\sigma,-,\alpha}| |\chi_{-\mathbf{k}'-\mathcal{Q},\sigma,-,\alpha}^*| |\chi_{\mathbf{k}',\sigma,-,\alpha}^*| \quad (\text{A10}) \\ &< NU \int \frac{d^2 \mathbf{k}}{(2\pi)^2} \int \frac{d^2 \mathbf{k}'}{(2\pi)^2} |A_{\mathbf{k}}^{(\mathcal{Q})}| |A_{\mathbf{k}'}^{(\mathcal{Q})*}| \\ &\leq NU \int \frac{d^2 \mathbf{k}}{(2\pi)^2} |A_{\mathbf{k}}^{(\mathcal{Q})}|^2 \\ &= U. \end{aligned}$$

Due to the normalization of the eigenspinors, the assumption (2.8), and the inequality (A7),

$$\sum_{\alpha=A,B} |\chi_{-\mathbf{k}-\mathcal{Q},\sigma,-,\alpha}| |\chi_{\mathbf{k},\sigma,-,\alpha}| |\chi_{-\mathbf{k}'-\mathcal{Q},\sigma,-,\alpha}^*| |\chi_{\mathbf{k}',\sigma,-,\alpha}^*| < 1 \quad (\text{A11})$$

holds for almost all \mathbf{k}, \mathbf{k}' . This allows the use of the strict inequality in the third-last inequality from the chain of inequalities (A10).

The penultimate inequality from the chain of inequalities (A10) is a consequence of Hölder's inequality

$$\int \frac{d^2 \mathbf{k}}{(2\pi)^2} |A_{\mathbf{k}}^{(\mathcal{Q})}| \leq \left(\int \frac{d^2 \mathbf{k}}{(2\pi)^2} |A_{\mathbf{k}}^{(\mathcal{Q})}|^2 \right)^{1/2}. \quad (\text{A12})$$

The last inequality in the chain of inequalities (A10) follows from the representation

$$\int \frac{d^2 \mathbf{k}}{(2\pi)^2} |A_{\mathbf{k}}^{(\mathcal{Q})}|^2 = \frac{1}{N} \quad (\text{A13})$$

of the normalization (A1e) in the thermodynamic limit. In summary, we have shown that

$$\langle \Phi_{\sigma,\mathcal{Q}} | (H + N_e) | \Phi_{\sigma,\mathcal{Q}} \rangle > 0 \quad (\text{A14})$$

holds in the thermodynamic limit under the assumption (2.8). In other words, the many-body gap

$$\Delta_{\sigma,\mathcal{Q}} := \langle \Phi_{\sigma,\mathcal{Q}} | H | \Phi_{\sigma,\mathcal{Q}} \rangle - \langle \Psi_{\sigma} | H | \Psi_{\sigma} \rangle > 0 \quad (\text{A15})$$

is non-vanishing under the assumption (2.8).

3. Proof of Eq. (2.10b)

We are now going to work exclusively with the single-particle eigenstates of the band Hamiltonian (2.2e).

We start with the completeness relation

$$\sum_{\mathbf{r} \in A} \sum_{\alpha=A,B} |\mathbf{r}, \alpha\rangle \langle \alpha, \mathbf{r}| = \mathbb{1} \quad (\text{A16a})$$

on the bipartite lattice $\Lambda = A \cup B$. The normalized Bloch states $|\varphi_{\mathbf{k},\sigma,\lambda}\rangle$ are defined in terms of the single-particle eigenstates $\chi_{\mathbf{k},\sigma,\lambda,\alpha}$ by their overlaps

$$\langle \alpha, \mathbf{r} | \varphi_{\mathbf{k},\sigma,\lambda} \rangle := \frac{e^{+i\mathbf{k}\cdot\mathbf{r}}}{\sqrt{N}} \chi_{\mathbf{k},\sigma,\lambda,\alpha} \quad (\text{A16b})$$

for any given (Ising) spin $\sigma = \uparrow, \downarrow$ and band $\lambda = \pm$. The normalization and phase factors are chosen so that the orthonormality condition

$$\langle \varphi_{\mathbf{k},\sigma,\lambda} | \varphi_{\mathbf{k},\sigma,\lambda'} \rangle = \delta_{\lambda,\lambda'} \quad (\text{A16c})$$

with $\lambda, \lambda' = \pm$ holds for any given wavenumber $\mathbf{k} \in \text{BZ}$ and any given spin $\sigma = \uparrow, \downarrow$. The overlap (A16b) is invariant under the translation $\mathbf{k} \rightarrow \mathbf{k} + \mathbf{Q}$ for any \mathbf{Q} that belongs to the reciprocal lattice of sublattice A owing to the periodicity

$$\chi_{\mathbf{k},\sigma,\lambda,\alpha} = \chi_{\mathbf{k}+\mathbf{Q},\sigma,\lambda,\alpha}. \quad (\text{A16d})$$

Wannier states are defined in terms of the Bloch states by the unitary transformation

$$|\psi_{\mathbf{z},\sigma,\lambda}\rangle := \frac{1}{\sqrt{N}} \sum_{\mathbf{k} \in \text{BZ}} e^{-i\mathbf{k}\cdot\mathbf{z}} |\varphi_{\mathbf{k},\sigma,\lambda}\rangle \quad (\text{A17a})$$

for any given unit cell of sublattice A labeled by \mathbf{z} and any given spin $\sigma = \uparrow, \downarrow$. The orthonormality (A16c) of the Bloch states thus carries over to the orthonormality

$$\langle \psi_{\mathbf{z},\sigma,\lambda} | \psi_{\mathbf{z},\sigma,\lambda'} \rangle = \delta_{\lambda,\lambda'} \quad (\text{A17b})$$

of the Wannier states for any given unit cell labeled by \mathbf{z} of sublattice A and any given spin $\sigma = \uparrow, \downarrow$. For any λ and α , the representation of the Wannier state on the bipartite lattice $\Lambda = A \cup B$ is the overlap

$$\begin{aligned} \psi_{\mathbf{r},\mathbf{z},\sigma,\lambda,\alpha} &:= \langle \mathbf{r}, \alpha | \psi_{\mathbf{z},\sigma,\lambda} \rangle \\ &= \frac{1}{\sqrt{N}} \sum_{\mathbf{k} \in \text{BZ}} e^{-i\mathbf{k}\cdot\mathbf{z}} \langle \mathbf{r}, \alpha | \varphi_{\mathbf{k},\sigma,\lambda} \rangle \\ &= \frac{1}{N} \sum_{\mathbf{k} \in \text{BZ}} e^{+i\mathbf{k}\cdot(\mathbf{r}-\mathbf{z})} \chi_{\mathbf{k},\sigma,\lambda,\alpha} \end{aligned} \quad (\text{A17c})$$

for any given unit cell of sublattice A labeled by \mathbf{z} and any given spin $\sigma = \uparrow, \downarrow$. The set of Wannier spinors

$$\psi_{\mathbf{r},\mathbf{z},\sigma,\lambda} = (\psi_{\mathbf{r},\mathbf{z},\sigma,\lambda,\alpha}) \quad (\text{A17d})$$

resolves the identity since

$$\sum_{\mathbf{r} \in A} \psi_{\mathbf{r},\mathbf{z},\sigma,\lambda}^\dagger \psi_{\mathbf{r},\mathbf{z}',\sigma,\lambda'} = \delta_{\mathbf{z},\mathbf{z}'} \delta_{\lambda,\lambda'} \quad (\text{A17e})$$

for any given spin $\sigma = \uparrow, \downarrow$. We want to estimate the profile in space of the Wannier states (A17a).

For that purpose, we consider the spread functional

$$\begin{aligned} R_{\sigma,\lambda}^{(2)} &:= \langle \psi_{\mathbf{z}=0,\sigma,\lambda} | \mathbf{r}^2 | \psi_{\mathbf{z}=0,\sigma,\lambda} \rangle \\ &\quad - | \langle \psi_{\mathbf{z}=0,\sigma,\lambda} | \mathbf{r} | \psi_{\mathbf{z}=0,\sigma,\lambda} \rangle |^2. \end{aligned} \quad (\text{A18})$$

Here, we are assuming, for simplicity, that there is only one band λ that is occupied. If more bands are occupied, we have to carry out a summation over all the occupied bands. Observe that by translational invariance $R_{\sigma,\lambda}^{(2)}$ is left unchanged under the global translation $\mathbf{r}, \mathbf{z} \rightarrow \mathbf{r} + \mathbf{R}, \mathbf{z} + \mathbf{R}$ for any lattice vector \mathbf{R} . Hence, the choice $\mathbf{z} = 0$ in Eq. (A18) can be done without loss of generality.

We rewrite Eq. (A18), following Ref. [12], as

$$R_{\sigma,\lambda}^{(2)} := R_{1|\sigma,\lambda}^{(2)} + \tilde{R}_{\sigma,\lambda}^{(2)}, \quad (\text{A19a})$$

$$\begin{aligned} R_{1|\sigma,\lambda}^{(2)} &:= \langle \psi_{\mathbf{z}=0,\sigma,\lambda} | \mathbf{r}^2 | \psi_{\mathbf{z}=0,\sigma,\lambda} \rangle \\ &\quad - \sum_{\mathbf{z}'} | \langle \psi_{\mathbf{z}=0,\sigma,\lambda} | \mathbf{r} | \psi_{\mathbf{z}',\sigma,\lambda} \rangle |^2, \end{aligned} \quad (\text{A19b})$$

$$\tilde{R}_{\sigma,\lambda}^{(2)} := \sum_{\mathbf{z}' \neq \mathbf{0}} | \langle \psi_{\mathbf{z}=0,\sigma,\lambda} | \mathbf{r} | \psi_{\mathbf{z}',\sigma,\lambda} \rangle |^2. \quad (\text{A19c})$$

Both $R_{1|\sigma,\lambda}^{(2)}$ and $\tilde{R}_{\sigma,\lambda}^{(2)}$ are non-negative quantities that can be expressed in terms of \mathbf{k} -space summations as follows. First,

$$\begin{aligned} R_{1|\sigma,\lambda}^{(2)} &= \sum_{j=x,y} \frac{1}{N} \sum_{\mathbf{k} \in \text{BZ}} \left[\left(\partial_{k_j} \chi_{\mathbf{k},\sigma,\lambda}^\dagger \right) \left(\partial_{k_j} \chi_{\mathbf{k},\sigma,\lambda} \right) - \left(\partial_{k_j} \chi_{\mathbf{k},\sigma,\lambda}^\dagger \chi_{\mathbf{k},\sigma,\lambda} \right) \left(\chi_{\mathbf{k},\sigma,\lambda}^\dagger \partial_{k_j} \chi_{\mathbf{k},\sigma,\lambda} \right) \right] \\ &= \sum_{j=x,y} \frac{1}{N} \sum_{\mathbf{k} \in \text{BZ}} \left[\langle \partial_{k_j} \chi_{\mathbf{k},\sigma,\lambda} | \partial_{k_j} \chi_{\mathbf{k},\sigma,\lambda} \rangle - \langle \partial_{k_j} \chi_{\mathbf{k},\sigma,\lambda} | \chi_{\mathbf{k},\sigma,\lambda} \rangle \langle \chi_{\mathbf{k},\sigma,\lambda} | \partial_{k_j} \chi_{\mathbf{k},\sigma,\lambda} \rangle \right] \\ &= \sum_{j=x,y} \frac{1}{N} \sum_{\mathbf{k} \in \text{BZ}} \langle \partial_{k_j} \chi_{\mathbf{k},\sigma,\lambda} | (\mathbb{1} - | \chi_{\mathbf{k},\sigma,\lambda} \rangle \langle \chi_{\mathbf{k},\sigma,\lambda} |) | \partial_{k_j} \chi_{\mathbf{k},\sigma,\lambda} \rangle \\ &\equiv \sum_{j=x,y} \frac{1}{N} \sum_{\mathbf{k} \in \text{BZ}} \langle \partial_{k_j} \chi_{\mathbf{k},\sigma,\lambda} | Q_{\mathbf{k},\sigma,\lambda} | \partial_{k_j} \chi_{\mathbf{k},\sigma,\lambda} \rangle \\ &= \frac{1}{N} \sum_{\mathbf{k} \in \text{BZ}} \text{tr} [g_{\mathbf{k},\sigma,\lambda}], \end{aligned} \quad (\text{A20a})$$

where

$$Q_{\mathbf{k},\sigma,\lambda} := \mathbb{1} - |\chi_{\mathbf{k},\sigma,\lambda}\rangle\langle\chi_{\mathbf{k},\sigma,\lambda}|, \quad (\text{A20b})$$

is the single-particle projector operator on all the Bloch states orthogonal to $|\chi_{\mathbf{k},\sigma,\lambda}\rangle$, the 2×2 matrix $[g_{\mathbf{k},\sigma,\lambda}]$ has the components

$$g_{\mathbf{k},\sigma,\lambda|i,j} := \text{Re} \left[\langle \partial_{k_i} \chi_{\mathbf{k},\sigma,\lambda} | Q_{\mathbf{k},\sigma,\lambda} | \partial_{k_j} \chi_{\mathbf{k},\sigma,\lambda} \rangle \right], \quad (\text{A20c})$$

labeled by the Euclidean indices $i, j \in \{x, y\}$ of two-dimensional space, and tr denotes the trace over $i, j \in \{x, y\}$. Second,

$$\tilde{R}_{\sigma,\lambda}^{(2)} = \sum_{j=x,y} \frac{1}{N} \sum_{\mathbf{k}} \left(A_{\mathbf{k},\sigma,\lambda|j} - \bar{A}_{\sigma,\lambda|j} \right)^2, \quad (\text{A21a})$$

where

$$A_{\mathbf{k},\sigma,\lambda|j} := i \langle \chi_{\mathbf{k},\sigma,\lambda} | \partial_{k_j} \chi_{\mathbf{k},\sigma,\lambda} \rangle, \quad (\text{A21b})$$

and

$$\bar{A}_{\sigma,\lambda|j} := \frac{1}{N} \sum_{\mathbf{k}} A_{\mathbf{k},\sigma,\lambda|j} \quad (\text{A21c})$$

denote the Berry connection and the average of the Berry connection, respectively. Under the gauge transformation

$$|\chi_{\mathbf{k},\sigma,\lambda}\rangle \rightarrow e^{i\varphi_{\mathbf{k}}} |\chi_{\mathbf{k},\sigma,\lambda}\rangle, \quad (\text{A22})$$

it can be shown that $R_{1|\sigma,\lambda}^{(2)}$ remains invariant while $\tilde{R}_{\sigma,\lambda}^{(2)}$ does not.

We will now establish a lower bound on the gauge invariant quantity $R_{1|\sigma,\lambda}^{(2)}$. To this end, we notice that, since $Q_{\mathbf{k},\sigma,\lambda}$ is a projection operator with eigenvalues 0, 1, then, for any single-particle state $|\Psi_{\mathbf{k},\sigma,\lambda}\rangle$, it follows that

$$0 \leq \langle \Psi_{\mathbf{k},\sigma,\lambda} | Q_{\mathbf{k},\sigma,\lambda} | \Psi_{\mathbf{k},\sigma,\lambda} \rangle. \quad (\text{A23})$$

In particular, if we choose

$$|\Psi_{\pm,\mathbf{k},\sigma,\lambda}\rangle := |\partial_{k_x} \chi_{\mathbf{k},\sigma,\lambda}\rangle \pm i |\partial_{k_y} \chi_{\mathbf{k},\sigma,\lambda}\rangle, \quad (\text{A24})$$

the inequality (A23) delivers

$$\text{tr} [g_{\mathbf{k},\sigma,\lambda}] \geq \mp i \left(\langle \partial_{k_x} \chi_{\mathbf{k},\sigma,\lambda} | \partial_{k_y} \chi_{\mathbf{k},\sigma,\lambda} \rangle - \langle \partial_{k_y} \chi_{\mathbf{k},\sigma,\lambda} | \partial_{k_x} \chi_{\mathbf{k},\sigma,\lambda} \rangle \right). \quad (\text{A25})$$

Summing (A25) over \mathbf{k} and taking the thermodynamic limit $N \rightarrow \infty$, delivers

$$\begin{aligned} R_{1|\sigma,\lambda}^{(2)} &= \frac{A_c}{(2\pi)^2} \int_{\text{BZ}} d^2\mathbf{k} \text{tr} [g_{\mathbf{k},\sigma,\lambda}] \\ &\geq \pm \frac{A_c}{2\pi} \int_{\text{BZ}} \frac{d^2\mathbf{k}}{2\pi i} \left[\langle \partial_{k_x} \chi_{\mathbf{k},\sigma,\lambda} | \partial_{k_y} \chi_{\mathbf{k},\sigma,\lambda} \rangle - \langle \partial_{k_y} \chi_{\mathbf{k},\sigma,\lambda} | \partial_{k_x} \chi_{\mathbf{k},\sigma,\lambda} \rangle \right] \\ &= \pm \frac{A_c}{2\pi} C_{\sigma,\lambda}, \end{aligned} \quad (\text{A26})$$

where A_c is the area of the unit cell of sublattice A and $C_{\sigma,\lambda}$ are the spin- and band-resolved Chern numbers. Since $R_{1|\sigma,\lambda}^{(2)} \geq 0$, it then follows

$$R_{1|\sigma,\lambda}^{(2)} \geq \frac{A_c}{2\pi} |C_{\sigma,\lambda}|, \quad (\text{A27})$$

as a lower bound, proportional to the band Chern number, on the gauge invariant part of spread of the Wannier states (A17a). It was shown in Ref.[12] that, in the topological phase of the Haldane model³, $R_{1|\sigma,\lambda}^{(2)}$ is finite while $\tilde{R}_{\sigma,\lambda}^{(2)}$ displays a logarithmic divergence which is related to the non-zero Chern number of the bands.

Appendix B: Competing Phases in the Hubbard model

Any translationally invariant electronic single-particle Hamiltonian is described in momentum space by the dispersions and Bloch eigenfunctions of its bands. Given the hopping amplitudes of a tight-binding model in position space, the dispersions and Bloch eigenfunctions are uniquely determined. Once interactions are included, the many-body ground state of the model depends crucially on the properties of the dispersions (bandwidths; shapes of Fermi surface, e.g., nesting; ...) and the properties of the Bloch states or Wannier states (Chern numbers, localization in position space, ...). The power of our approach, the flattening of the band with the factor $w_{\mathbf{k}}$ from Eq. (2.2), is to disentangle the properties of the dis-

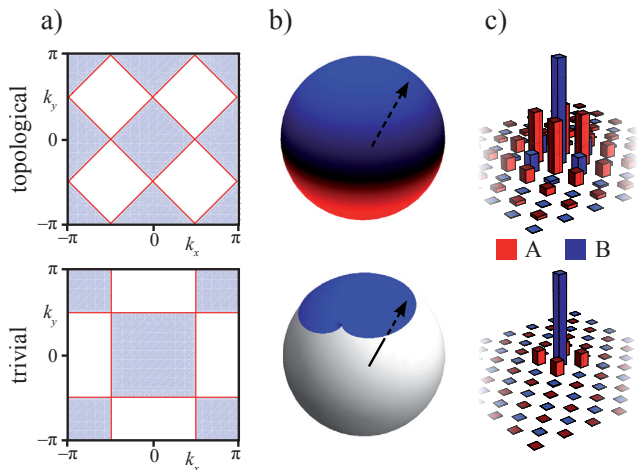


FIG. 3. (Color online) Comparison of the topological (top; $t_2 = 1/\sqrt{2}$, $\mu_s = 0$) and non-topological (bottom; $t_2 = 0$, $\mu_s = 1/\sqrt{2}$) single-particle model. (a) The shaded area represents the Fermi sea of the lower band at the commensurate filling fraction $N_e = N$ when $\kappa < 1$. (b) The eigenspinor $\chi_{\mathbf{k},\sigma}$, when interpreted as a point on the surface of the unit sphere, swipes out the full surface of this sphere (a small portion of this sphere near one pole) as \mathbf{k} takes values everywhere in the BZ for the topological (non-topological) band structure. (c) The spread of the Wannier states (A17c) in real space indicates their delocalized (localized) character for the topological (non-topological) band structure.

persions from those of the spinors to some extent and to study their effects individually.

1. Possible phases

Let us list the anticipated ground states for some limiting properties of the spinors and the dispersions for $N_e = N$ electrons when the two pairs of bands are separated by a gap in the absence of interactions.

1. *(Almost) flat band and sublattice-polarized spinors.* If the band is completely flat ($\kappa = 1$), the ground state is macroscopically degenerate in the absence of interactions. Moreover, when the Bloch states are fully sublattice polarized, i.e., when $\chi_{\mathbf{k}}^\dagger = (1, 0)$ say, then the kinetic energy becomes diagonal in position space [$\psi_{\mathbf{r},\mathbf{z},\sigma,-}^\dagger = \delta_{\mathbf{r},\mathbf{z}}(1, 0)$]. Hence, any state with no less and no more than one electron per site on sublattice *A* will be a ground state of the Hamiltonian, regardless of the spin-configuration of the electrons. Therefore, the ground state remains macroscopically degenerate, in spite of the presence of the Hubbard interaction. This degeneracy can be lifted by introducing a small but finite bandwidth, while keeping the full sublattice polarization of the spinors intact. Then, the low-energy degrees of freedom of the model map on the conventional one-band Hubbard model at half filling

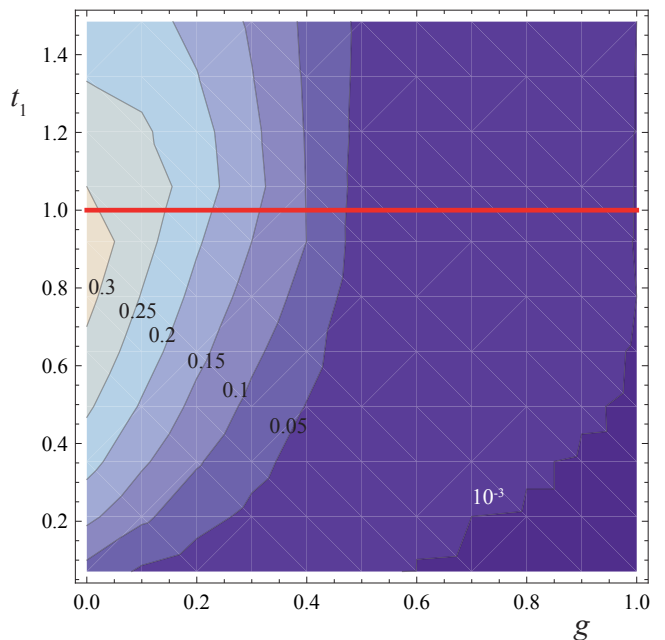


FIG. 4. (Color online) Numerical exact diagonalization results for flat bands $\kappa = 1$ for the system size $L_x = L_y = 25$ at the commensurate filling fraction $N_e = N$. Plotted is the value of the many-body excitation gap Δ/U between the energy of the fully spin polarized state $S = N$ and the lowest energy state in the sector with one spin flipped $S = N - 2$ as a function of $g := (2/\pi)\arctan|\mu_s/t_2|$ and the nearest-neighbor hopping parameter t_1 . The thick red line corresponds to the parameter choice made for the plot in Fig. 1 of the Letter. As discussed in the text, the spinors of the Bloch band become fully sublattice polarized in the limit $t_1 \rightarrow 0$ and the ferromagnetic ground state becomes degenerate in energy with states from other spin sectors ($\Delta \rightarrow 0$).

with $t \ll U$, i.e., on the t - J model. An antiferromagnetic ground state will be selected. An alternative way to lift the macroscopic degeneracy is to add longer range interactions, in which case other ground states may be stabilized¹⁸. Note that the fully sublattice polarized spinors discussed here imply that the non-interacting model is topologically trivial.

2. *Flat band and not sublattice polarized spinors.* As was shown in the Letter, if the spinors are sufficiently spread between the two sublattices, i.e., if condition (2.8) is met, the ground state in the limit of flat bands is an Ising ferromagnet with full spin polarization.
3. *Strongly dispersing unnested band.* For a strongly dispersing band without a nested Fermi surface, the Fermi liquid ground state is expected to be stable against sufficiently small repulsive Hubbard interactions. One generic instability at *finite* interaction strength is Stoner ferromagnetism which, in contrast to the flat band ferromagnetism, does not

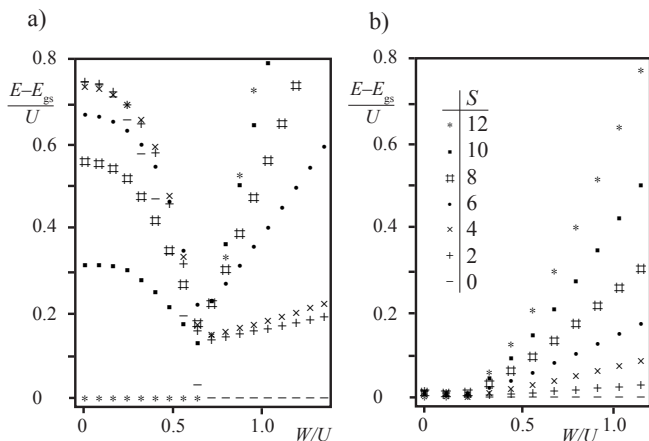


FIG. 5. Numerical exact diagonalization results at the commensurate filling fraction $N_e = N$ as a function of the band width W for $L_x = 3$, $L_y = 4$. Plotted is the energy of the lowest state in different sectors of total spin S (in units of $\hbar/2$) measured with respect to the ground state energy. (a) Topological phase with $\mu_s = 0$, $t_2 = 1/\sqrt{2}$. The ground state is gaped and fully spin-polarized for $W/U < 0.7$, while it is unpolarized for $W/U > 0.7$. (b) Topological trivial phase with $\mu_s = 1/\sqrt{2}$, $t_2 = 0$. The unpolarized ground state appears already for very small values of W/U .

automatically yield full spin polarization.

4. *Strongly dispersing nested band.* If the Fermi surface is nested, arbitrary small Hubbard interactions destabilize the Fermi liquid ground state toward an antiferromagnet.

2. Realization in our model

The shape of the Wannier states is controlled by the parameters t_2 and μ_s in our model. If they are topologically non-trivial ($|t_2/\mu_s| > 1$), the Wannier states are relatively wide spread over several lattice sites as illustrated in Fig. 3 (c) and by Eq. (A27). In contrast, deep in the topological trivial regime $|t_2/\mu_s| \ll 1$, the Wannier states become more and more localized. Intuitively, their localization is more pronounced the smaller the area covered by the spinor $\chi_{\mathbf{k},\sigma,\lambda}$ on the unit sphere as \mathbf{k} takes values everywhere in the BZ [Fig. 3 (b)].

In our model, the full sublattice polarization is achieved by taking the limit $t_1 \rightarrow 0$ while $|t_2/\mu_s| < 1$ (this limit is not shown in the Figures of the Letter). In the case of flat bands, this limit is the transition from phase 2 to phase 1 from the list above. As shown in Fig. 4, the many-body gap Δ of the flatband ferromagnetism collapses regardless of the value taken by the ratio $|t_2/\mu_s|$ as $t_1 \rightarrow 0$. The lowest energy states of each spin sector become degenerate in this limit as the full $SU(2)$ spin-1/2 symmetry of the Hubbard interaction is recovered in the limit $t_1 \rightarrow 0$.

We studied the effect of finite band width both in the topological trivial ($|t_2/\mu_s| < 1$) and non-trivial sector ($|t_2/\mu_s| > 1$) sector (Fig. 5). In both cases, an interpolation between the phases 2 and 4 follows from changing the ratio W/U [Fig. 3(a) illustrates the nesting of the Fermi surfaces for the parameters chosen.]. The difference between topological non-trivial and trivial case is quantitative: While the many-body gap Δ protects the Ising ferromagnetic state against the effect of a sizable band width in the former case, the transition to the antiferromagnetic state occurs already for very small W/U in the latter.

¹ P. A. Lee, N. Nagaosa, and X.-G. Wen, Rev. Mod. Phys. **78**, 17 (2006).
² *The Quantum Hall Effect*, edited by R. E. Prange and S. M. Girvin (Springer, New York, 1987).
³ F. D. M. Haldane, Phys. Rev. Lett. **61**, 2015 (1988).
⁴ T. Neupert, L. Santos, C. Chamon, and C. Mudry, Phys. Rev. Lett. **106**, 236804 (2011).
⁵ D. N. Sheng, Z. Gu, K. Sun, and L. Sheng, Nature Communications **2**, 389 (2011).
⁶ Y.-F. Wang, Z.-C. Gu, C.-D. Gong, D. N. Sheng, arXiv:1103.1686 (unpublished).
⁷ N. Regnault and B. A. Bernevig, arXiv:1105.4867 (unpublished).
⁸ D. Xiao, W. Zhu, Y. Ran, N. Nagaosa, and S. Okamoto, arXiv:1106.4296 (unpublished).
⁹ Fa Wang and Ying Ran, arXiv:1109.3435 (unpublished).
¹⁰ B. A. Bernevig and S.-C. Zhang, Phys. Rev. Lett. **96**,

106802 (2006).
¹¹ H. Katsura, I. Maruyama, A. Tanaka, and H. Tasaki, Europhys Lett. **91**, 57007 (2010) and references therein.
¹² T. Thonhauser and David Vanderbilt, Phys. Rev. B **74** 235111 (2006).
¹³ See for instance K. von Klitzing, Phil. Trans. R. Soc. A **363**, 2203 (2005).
¹⁴ J. Matthews and M. E. Cage, J. Res. Natl. Inst. Stand. Technol. **110**, 497 (2005).
¹⁵ R. W. Rendell and S. M. Girvin, Phys. Rev. B **23**, 6610 (1981).
¹⁶ R. A. Matula, J. Phys. Chem. Ref. Data **8**, 1147 (1979).
¹⁷ For reviews of DMFT and MPS methods, see respectively A. Georges, G. Kotliar, W. Krauth and M. Rozenberg, Rev. of Mod. Phys. **68**, 13(1996) and J. I. Cirac and F. Verstraete, J. Phys. A: Math. Theor. **42**, 504004 (2009).
¹⁸ T. Neupert, L. Santos, S. Ryu, C. Chamon, and C. Mudry, arXiv:1106.3989 (unpublished).